

Krishna Prasad MADASU ¹, Priya SARKAR ¹

Couple stress fluid past a sphere embedded in a porous medium

Received 1 September 2021, Revised 10 November 2021, Accepted 14 November 2021, Published online 1 December 2021

Keywords: sphere, couple stress fluid, saturated porous medium, Brinkman's equation, drag force

This paper concerns the analytical investigation of the axisymmetric and steady flow of incompressible couple stress fluid through a rigid sphere embedded in a porous medium. In the porous region, the flow field is governed by Brinkman's equation. Here we consider uniform flow at a distance from the sphere. The boundary conditions applied on the surface of the sphere are the slip condition and zero couple stress. Analytical solution of the problem in the terms of stream function is presented by modified Bessel functions. The drag experienced by an incompressible couple stress fluid on the sphere within the porous medium is calculated. The effects of the slip parameter, the couple stress parameter, and permeability on the drag are represented graphically. Special cases of viscous flow through a sphere are obtained and the results are compared with earlier published results.

1. Introduction

The fluid flow through porous media has been an interesting area of research for the last five decades. Many industrial, hydrologists, geologists, and several other researchers have been attracted to study the flow behavior in a porous medium, because it is related to many fields, like the shale gas extraction and enhanced oil recovery, soil contamination, heat exchange, separation, the processes of filtration, and catalyst support in the industry. In macroscopic scale, the fluid flow in an isotropic and homogeneous porous medium is governed by Darcy's law [1] or Brinkman's equations [2]. In Darcy's law, porosity is very low. But one encounters

✉ Krishna Prasad MADASU, emails: madaspra.maths@nitrr.ac.in, kpm973@gmail.com

¹Department of Mathematics, National Institute of Technology, Raipur-492010, Chhattisgarh, India; ORCID: K.P.M. 0000-0002-1819-3651, P.S. 0000-0003-1902-2747



© 2022. The Author(s). This is an open-access article distributed under the terms of the Creative Commons Attribution-NonCommercial-NoDerivatives License (CC BY-NC-ND 4.0, <https://creativecommons.org/licenses/by-nc-nd/4.0/>), which permits use, distribution, and reproduction in any medium, provided that the Article is properly cited, the use is non-commercial, and no modifications or adaptations are made.

a problem with high porosity and a large tangential rate, because Darcy's law is incapable to solve such a problem. To solve this problem, Brinkman's equation is used.

Davis and Stone [3] investigated the flow of viscous fluid through the beds of porous particles. They found that when permeability increases, the drag force decreases because high permeability offers less resistance to flow through the porous interior. The flow of a Newtonian fluid through a sphere embedded in a porous medium was studied by Barman [4]. Pop and Ingham [5] investigated Brinkman's model for a flow past a sphere implanted in a porous medium. The flow past an axisymmetric body implanted in a porous medium was examined, based on Brinkman's equation, by Srinivasacharya and Murthy [6]. Grosan et al. [7] obtained analytical results for a 2-D viscous fluid flow through a sphere implanted in another porous medium based on the Brinkman's model. Deo and Gupta [8] studied the drag force of an incompressible viscous fluid through a porous sphere implanted in another porous medium. The Newtonian fluid flow past a sphere and a cylinder in a Brinkman's porous medium with the Navier boundary condition was investigated by Leontev [9]. El-Sapa [10] obtained an analytical solution for thermophoresis of a particle located at the central position of a spherical cavity filled with a Brinkman's porous medium. Faltas et al. [11] examined the mobilities of a spherical particle straddling the interface of a semi-infinite Brinkman flow.

Madasu and Srinivasacharya [12] investigated the flow of micropolar fluid through a sphere and a cylinder embedded in a Brinkman porous medium. They observed that the drag in the micropolar case is higher than the drag in the viscous fluid. Jaiswal [13] studied the creeping flow over Reiner-Rivlin liquid sphere embedded in a micropolar fluid saturated in the Brinkman porous medium. Ramalakshmi and Shukla [14] examined the drag force on a fluid sphere implanted in a porous medium with a solid core based on Brinkman's equation. Madasu and Bucha [15] studied the effect of MHD on micropolar fluid flow through a sphere implanted in a Brinkman's porous medium.

Stokes [16, 17] introduced the theory of couple stress fluid which describes the behavior of fluids with microstructure. The couple stress fluid model is used to study the blood flow in the microcirculation [18]. Khan et al. [19] obtained an approximate solution for the couple stress fluid with expanding or contracting porous channel. Srinivasacharya et al. [20] studied a non-Darcy porous medium saturated in a couple stress fluid with the effect of Soret and Dufour. Devakar et al. [21] investigated the analytical solution of the Couette flow and the Poiseuille flow for the couple stress fluid using the slip condition. Srinivasacharya et al. [22] studied a couple stress fluid flow between two parallel porous plates. They found that, when the couple stress fluid parameter increases, its velocity decreases. Ashmawy [23] applied the slip boundary condition to obtain the drag force acting on a particle in the couple stress fluid. He found that the resistance of a couple stress fluid exceeds the resistance of a viscous fluid. Aparna et al. [24] studied a steady oscillating flow

of a couple stress fluid through a sphere. Adesanya et al. [25] performed the entropy generation analysis for a steady couple stress fluid flow through the Brinkman's porous material. Hassan [26] investigated reactive hydromagnetic couple stress fluid flow through a porous medium. Abdelsalam et al. [27] studied the effect of electro-magnetically modulated self-propulsion of swimming sperms via cervical canal. Bhatti et al. [28] investigated the intra-uterine flow with small suspended particles under the impact of heat transfer.

In the Stokes theory, the spherical part of the couple stress tensor is indeterminate, and the presence of body couples is neglected also in the constitutive relations. These problems have been solved by Hadjesfandiari et al. [29–32]. Recently, Hadjesfandiari and Dargush [30] have developed the consistent couple stress theory. According to their theory, the couple stress tensor is skew-symmetric.

In the last century, several studies have shown that the no-slip condition might not always hold, and at the solid boundary layers and, fluid slippage might occur. A general boundary condition that allows the fluid slip at a solid boundary was investigated by Navier [33]. The slip boundary condition specifies that, on the surface, the tangential fluid velocity of the solid is directly proportional to the shear stress at that point. The slip coefficient is the constant of proportionality which depends on properties of fluid and solid surfaces. Eldesoky et al. [34] examined the influence of slip, heat transfer, and magnetic field on a particulate fluid suspension in a catheterized wavy tube. Bhatti and Abdelsalam [35] examined the slip effect on entropy of a magnetized particle fluid motion through a porous channel. El-Sapa and Alsudais [36] studied the slip effect on two rigid spheres implanted in porous media in the presence of magnetic field. Madasu et al. [37] investigated the slow motion past a spheroid implanted in a Brinkman medium with slip condition.

The present article extends the work done by Leontev [9] by examining the impact of slip on a sphere implanted in a Brinkman's porous medium saturated by a couple stress fluid. The flow is steady and axisymmetric. On the surface of the sphere, we applied the slip condition and the vanishing couple stress condition. The pressure expression and the stream function are obtained. The drag exerted on the rigid sphere is calculated and special known cases are deduced. The influence of slip, couple stress, couple stress viscosity ratio, and permeability parameters on drag are studied graphically.

2. Mathematical formulation

Fig. 1 shows the incompressible couple stress fluid past a solid sphere of radius $r = a$ immersed in a porous medium. An uniform flow U is far away from the sphere. In the permeable region, the flow is governed by Brinkman's equation. The assumed Reynolds number is very small, so that, the inertial terms in the fluid momentum are neglected and only viscous terms are present.

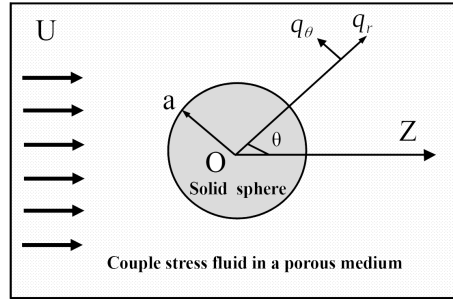


Fig. 1. Geometry of couple stress fluid past a slip sphere in a porous medium

The governing equations of a flow of an incompressible couple stress fluid past a sphere implanted in a porous region based on Brinkman's equation are given by [16, 17, 25, 26]

$$\nabla \cdot \vec{q} = 0, \quad (1a)$$

$$\nabla p + \frac{\mu}{k} \vec{q} + \mu \nabla \times \nabla \times \vec{q} + \eta \nabla \times \nabla \times \nabla \times \vec{q} = 0, \quad (1b)$$

where \vec{q} is the velocity, k is the permeability, p is the pressure, μ is the viscosity coefficient, and η and η' are the coefficients of couple stress viscosity.

The material constants are [17],

$$\mu \geq 0, \quad \eta \geq 0, \quad \eta \geq \eta'. \quad (2)$$

The constitutive equation of stress and couple stress are [17], respectively

$$t_{ij} = -p\delta_{ij} + 2\mu d_{ij} - \frac{1}{2} e_{ijk} m_{sk,s}, \quad (3)$$

$$m_{ij} = m\delta_{ij} + 4(\eta\omega_{j,i} + \eta'\omega_{i,j}), \quad (4)$$

where $\omega_{j,i}$ is the spin tensor.

The deformation rate tensor d_{ij} is written as [17]

$$d_{ij} = \frac{1}{2}(q_{i,j} + q_{j,i}). \quad (5)$$

The ω vorticity vector is defined as [23]

$$\omega = \frac{1}{2} e_{ijk} q_{k,j}. \quad (6)$$

The Kronecker delta and the alternating tensor are δ_{ij} and e_{ijk} , respectively.

$$\delta_{ij} = \begin{cases} 0, & \text{for } i \neq j, \\ 1, & \text{for } i = j. \end{cases}$$

$$e_{ijm} = \begin{cases} 1, & \text{for } e_{123}, e_{231}, e_{312}, \\ -1, & \text{for } e_{132}, e_{321}, e_{213}, \\ 0, & \text{otherwise.} \end{cases}$$

For dimensionless governing equations, we used the following non-dimensional variables

$$\vec{q} = U\tilde{q}, \quad p = \frac{\mu U}{a}\tilde{p}, \quad \nabla = \frac{\tilde{\nabla}}{a}. \quad (7)$$

Substituting Eq. (7) in Eq. (1) and then dropping the tildes, we get

$$\nabla p + \alpha^2 \vec{q} + \nabla \times \nabla \times \vec{q} + \frac{1}{\lambda^2} \nabla \times \nabla \times \nabla \times \vec{q} = 0, \quad (8)$$

where $\alpha^2 = \frac{a^2}{k}$ is the permeability parameter and $\lambda = \sqrt{\frac{\mu a^2}{\eta}}$ is the length-dependent parameter of the couple stress fluid. If λ approaches infinity, Eq. (8) represents the modified Stokes equation for non-polar fluid.

The spherical polar coordinate system (r, θ, ϕ) has the origin at the center of the sphere. Since the fluid flow is axially symmetric, all the quantities are independent of ϕ .

Now, the velocity vector \vec{q} is defined as

$$\vec{q} = (q_r(r, \theta), q_\theta(r, \theta), 0). \quad (9)$$

The stream function satisfies the continuity equation, and we define velocity components in terms of the stream function

$$q_r = -\frac{1}{r^2 \sin \theta} \frac{\partial \psi}{\partial \theta}, \quad q_\theta = \frac{1}{r \sin \theta} \frac{\partial \psi}{\partial r}. \quad (10)$$

Eliminating the pressure term, we get

$$E^2(E^2 - \xi_1^2)(E^2 - \xi_2^2)\psi = 0, \quad (11)$$

where $E^2 = \frac{\partial^2}{\partial r^2} + \frac{1}{r^2} \frac{\partial^2}{\partial \theta^2} - \frac{\cot \theta}{r^2} \frac{\partial}{\partial \theta}$ is the Stokes operator,

$$\xi_1^2 = \frac{\lambda^2 + \lambda \sqrt{\lambda^2 - 4\alpha^2}}{2},$$

$$\xi_2^2 = \frac{\lambda^2 - \lambda \sqrt{\lambda^2 - 4\alpha^2}}{2}.$$

3. Solution of the problem

The solution of the sixth-order linear partial differential Eq. (11) is obtained by using the method of separation of variables satisfying the condition of uniform velocity far away from the slip sphere, and is given by

$$\psi = \frac{1}{2} \left(r^2 + \frac{A}{r} + B\sqrt{r}K_{3/2}(\xi_1 r) + C\sqrt{r}K_{3/2}(\xi_2 r) \right) \sin^2 \theta, \quad (12)$$

where $K_{3/2}(\xi_1 r)$ and $K_{3/2}(\xi_2 r)$ are modified Bessel's function of the second kind of order $3/2$. A, B, and C are arbitrary constants.

Substituting Eq. (12) into Eq. (10), we get

$$q_r = - \left[1 + Ar^{-3} + Br^{-\frac{3}{2}}K_{3/2}(\xi_1 r) + Cr^{-\frac{3}{2}}K_{3/2}(\xi_2 r) \right] \cos \theta, \quad (13)$$

$$q_\theta = \frac{1}{2} \left[2 - Ar^{-3} - Br^{-\frac{3}{2}} (K_{3/2}(\xi_1 r) + \xi_1 r K_{1/2}(\xi_1 r)) - Cr^{-\frac{3}{2}} (K_{3/2}(\xi_2 r) + \xi_2 r K_{1/2}(\xi_2 r)) \right] \sin \theta, \quad (14)$$

The non-zero vorticity vector is

$$\omega_\phi = \frac{1}{4} \left\{ Br^{-\frac{1}{2}}\xi_1^2 K_{3/2}(\xi_1 r) + Cr^{-\frac{1}{2}}\xi_2^2 K_{3/2}(\xi_2 r) \right\} \sin \theta, \quad (15)$$

The expression for pressure is

$$p = \alpha^2 \left(r - \frac{A}{2r^2} \right) \cos \theta. \quad (16)$$

4. Boundary conditions

On the surface of the sphere, we require three boundary conditions to find the unknowns A, B, and C. We assume impenetrability of the surface, and presuppose that the tangential velocity of the couple stress fluid relative to the solid at a point on its surface is proportional to the tangential stress prevailing at that point [33]. The latter is known as the slip boundary condition introduced by Navier in 1823. Recently, some researchers have studied the slip effect on the flow between porous channels [36, 37].

Another boundary condition for the couple stress fluid is zero couple stress at the boundary [23]. In addition, the normal velocity components vanish [38]. We have:

- The impenetrability condition on surface of sphere

$$q_r = 0, \quad (17)$$

- The slip boundary condition defined as

$$\beta_1 q_\theta = t_{r\theta}, \quad (18)$$

- The vanishing couple stress given as

$$m_{r\phi} = 0, \quad (19)$$

where β_1 is the slip coefficient of the sphere. The coefficient β_1 depends on the nature of the solid and fluid surface. In the limiting case of $\beta_1 = 0$, there is a perfect slip and the solid sphere acts like a spherical gas bubble. If $\beta_1 \rightarrow \infty$, we get the standard no-slip condition.

The expressions for stress and couple stress components are

$$t_{rr} = \left[-\alpha^2 \left(r - \frac{1}{2} Ar^{-2} \right) + 6Ar^{-4} + r^{-\frac{5}{2}} \left(6K_{3/2}(\xi_1 r) + 2\xi_1 r K_{1/2}(\xi_1 r) \right) B \right. \\ \left. + r^{-\frac{5}{2}} \left(6K_{3/2}(\xi_2 r) + 2\xi_2 r K_{1/2}(\xi_2 r) \right) C \right] \cos \theta, \quad (20)$$

$$t_{r\theta} = \frac{1}{2} \left[6Ar^{-4} + r^{-\frac{5}{2}} \left(\left(6 + r^2 \alpha^2 \right) K_{3/2}(\xi_1 r) + 2\xi_1 r K_{1/2}(\xi_1 r) \right) B \right. \\ \left. + r^{-\frac{5}{2}} \left(\left(6 + r^2 \alpha^2 \right) K_{3/2}(\xi_2 r) + 2\xi_2 r K_{1/2}(\xi_2 r) \right) C \right] \sin \theta, \quad (21)$$

$$m_{r\phi} = -r^{-\frac{3}{2}} \left[\left((2\eta + \eta') \xi_1^2 K_{3/2}(\xi_1 r) + \eta \xi_1^3 r K_{1/2}(\xi_1 r) \right) B \right. \\ \left. + \left((2\eta + \eta') \xi_2^2 K_{3/2}(\xi_2 r) + \eta \xi_2^3 r K_{1/2}(\xi_2 r) \right) C \right] \sin \theta, \quad (22)$$

$$m_{\phi r} = -r^{-\frac{3}{2}} \left[\left((\eta + 2\eta') \xi_1^2 K_{3/2}(\xi_1 r) + \eta' \xi_1^3 r K_{1/2}(\xi_1 r) \right) B \right. \\ \left. + \left((\eta + 2\eta') \xi_2^2 K_{3/2}(\xi_2 r) + \eta' \xi_2^3 r K_{1/2}(\xi_2 r) \right) C \right] \sin \theta, \quad (23)$$

$$m_{\theta\phi} = r^{-\frac{3}{2}} \left[\left((\eta - \eta') \xi_1^2 K_{3/2}(\xi_1 r) \right) B + \left((\eta - \eta') \xi_2^2 K_{3/2}(\xi_2 r) \right) C \right] \cos \theta. \quad (24)$$

Applying the boundary conditions, we have

$$A = -\frac{a^3 (\tau J_6 + \xi_4^2 J_3 J_7 - \xi_3^2 J_4 J_5)}{\Delta_1}, \quad (25)$$

$$B = \frac{3a^{\frac{3}{2}} \xi_4^2 J_1 J_{11}}{\Delta_1}, \quad (26)$$

$$C = -\frac{3a^{\frac{3}{2}} \xi_3^2 J_1 J_{12}}{\Delta_1}. \quad (27)$$

5. Drag force

The drag acting on the sphere in a porous medium is evaluated by the formula

$$F_z = 2\pi a^2 \int_0^\pi r^2 (t_{rr} \cos \theta - t_{r\theta} \sin \theta) \Big|_{r=a} \sin \theta d\theta, \quad (28)$$

substituting the values of the Eqs. (20) and (21) in the above formula, we obtain

$$F_z = \frac{2}{3} \pi \mu a U \alpha^2 \left(A - 2a^3 - 2a\sqrt{a} K_{3/2}(\xi_1 a) B - 2a\sqrt{a} K_{3/2}(\xi_2 a) C \right), \quad (29)$$

substituting the values of A, B, and C, we get

$$F_z = -\pi \mu a U \left[\frac{2a^3 \alpha^2 (\tau J_6 + \xi_4^2 J_3 J_7 - \xi_3^2 J_4 J_5)}{\Delta_1} \right]. \quad (30)$$

6. Special cases

Case 1: If $\lambda_1 \rightarrow \infty$ and $a = 1$ in Eq. (30), the drag force acting on a sphere embedded in a Brinkman's porous medium with effect of slip is obtained as

$$F_z = -2\pi \mu a U \left(\frac{(\alpha^2 + 3\alpha + 3)\beta_1 + \alpha^3 + 3\alpha^2 + 6\alpha + 6}{\beta_1 + \alpha + 3} \right). \quad (31)$$

It matches the result given by Madasu et al. [37] and El-Sapa et al. [39].

Case 2: In the absence of permeability ($\alpha = 0$ i.e., $\xi_1 = \lambda$, and $\xi_2 = 0$) in Eq. (30), the drag experienced by an incompressible couple stress fluid past a sphere is

$$F_z = -6\pi \mu a U \left(1 + \frac{\tau_1(\beta_2 + 1) - \lambda_1}{\tau_1 + \lambda_1(\beta_2 + 3)} \right), \quad (32)$$

where

$$\lambda_1 = a\lambda, \quad \tau_1 = \frac{\tau + 2}{\tau + \lambda_1 + 2}, \quad \beta_2 = \frac{a\beta_1}{\mu}.$$

This result is the same as in Ashmawy [23].

Case 3: If $\beta_2 \rightarrow \infty$ in Eq. (32), the drag force reduces to

$$F_z = -6\pi \mu a U \left(1 + \frac{\tau_1}{\lambda_1} \right). \quad (33)$$

Here, F_z exerted by couple stress fluid on the no-slip sphere is as that obtained by Stokes [40].

Case 4: If $\eta \rightarrow 0$ ($\lambda_1 \rightarrow \infty$) in Eq. (32), the drag force is

$$F_z = -6\pi\mu aU \left(\frac{\beta_2 + 2}{\beta_2 + 3} \right). \quad (34)$$

Here F_z is the force exerted by viscous fluid on a slip sphere.

Case 5: If $\eta \rightarrow 0$ and $\beta_2 \rightarrow \infty$ in Eq. (32), the drag force acting on no-slip sphere in a viscous fluid is

$$F_0 = -6\pi\mu aU. \quad (35)$$

Case 6: If $\tau = -1$, we get the drag force acting on the slip sphere in consistent couple stress fluid

$$F_z = -2\pi\mu aU \left(\frac{a\alpha^2 (\xi_4^2 J_3 J_{14} - \xi_3^2 J_4 J_{13})}{\Delta_2} \right). \quad (36)$$

Case 7: In the absence of permeability ($\alpha = 0$ i.e., $\xi_1 = \lambda$ and $\xi_2 = 0$) in Eq. (36), the drag experienced by the consistent couple stress fluid past a slip sphere is

$$F_z = -6\pi\mu aU \left(1 + \frac{(\beta_2 + 1) - \lambda_1(\lambda_1 + 1)}{1 + \lambda_1(\lambda_1 + 1)(\beta_2 + 3)} \right). \quad (37)$$

Case 8: If $\beta_2 \rightarrow \infty$ in Eq. (37), the drag force reduces to

$$D = -6\pi\mu aU \left(\frac{\lambda_1^2 + \lambda_1 + 1}{\lambda_1(\lambda_1 + 1)} \right). \quad (38)$$

This result agrees with the result obtained by Hadjesfandiari and Dargush [29].

7. Graphical results and discussion

The normalized drag D_N is the ratio of drag force F_z experienced by couple stress fluid in a porous medium to the drag force F_0 exerted by the no-slip sphere in a viscous fluid. The real parts of D_N are depicted graphically in Figs. 2-7 with the following parameters

- Couple stress parameter: λ ,
- Couple stress viscosity ratio parameter: τ ,
- Slip parameter: β_1 ,
- Permeability parameter: $k_1 \left(= \frac{1}{\alpha^2} = \frac{k}{a^2} \right)$.

According to the couple stress fluid theory, the range of τ is 0 to ∞ , while in the modified couple stress fluid theory, $\tau = -1$.

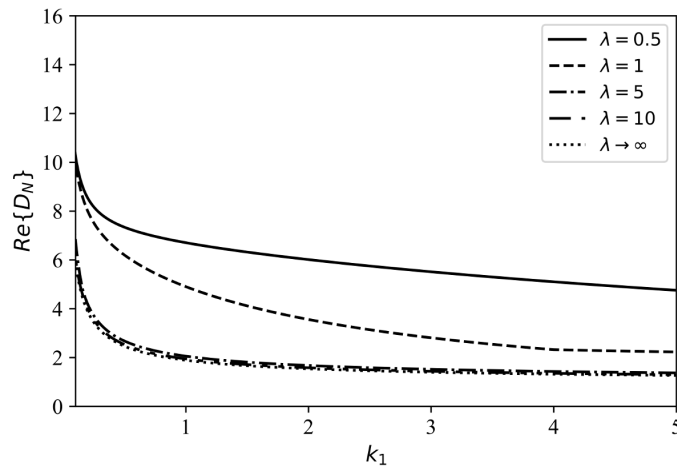


Fig. 2. Variation of real part of normalized drag D_N with k_1 for $\tau = 1, \beta_1 = 5$ and $a = 1$

Fig. 2 shows the variation of $Re(D_N)$ against the permeability parameter k_1 for varying values of the couple stress parameter λ . It is observed that, when the value of λ increases, the normalized drag force $Re(D_N)$ decreases with increasing value of k_1 .

From Fig. 3, one can notice that the couple stress parameter $\lambda \rightarrow \infty$, the fluid is viscous, and the drag force exerted by Newtonian fluid on the sphere is different from the drag force experienced by the couple stress fluid on the sphere.

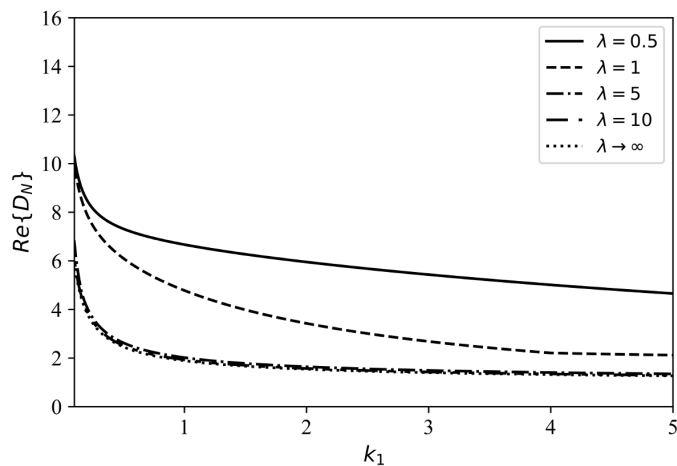


Fig. 3. Variation of real part of normalized drag D_N with k_1 for $\tau = 0, \beta_1 = 5$ and $a = 1$

The effects of τ and β_1 on the real part of the normalized drag force D_N are depicted in Fig. 4 and 5, respectively. It is shown that the drag force is slightly increased as the couple stress viscosity ratio parameter τ increases in Fig. 4.

When $\tau = -1$, the case represents the consistent couple stress fluid and $Re(D_N)$ decreases as k_1 increases. Fig. 5 shows that the drag force $Re(D_N)$ increases as the slip parameter β_1 increases. We notice that the drag acting on a no-slip sphere is higher than the drag acting on a slip sphere.

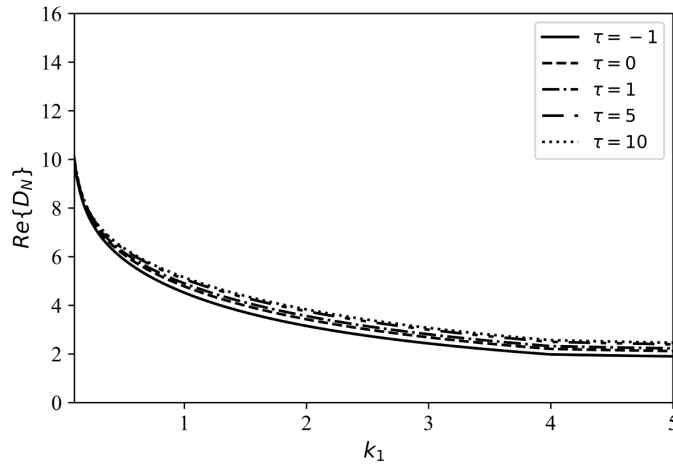


Fig. 4. Variation of real part of normalized drag D_N with k_1 for $\lambda = 1$, $\beta_1 = 5$ and $a = 1$

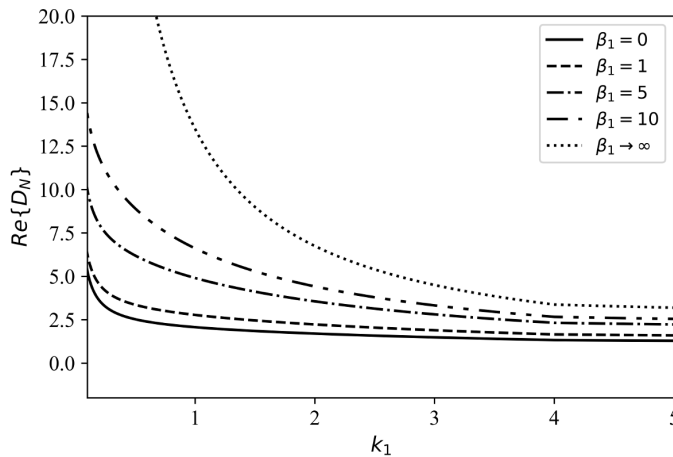


Fig. 5. Variation of real part of normalized drag D_N with k_1 for $\tau = 1$, $\lambda = 1$ and $a = 1$

Fig. 6 and 7 present the variation of the drag force $Re(D_N)$ against k_1 for varying values of the couple stress parameter λ and the slip parameter β_1 , respectively. For the consistent couple stress fluid, the normalized drag force $Re(D_N)$ decreases as λ increases in Fig. 6. Fig. 7 shows that, when slip parameter β_1 increases, the drag force $Re(D_N)$ also increases. For no-slip case $\beta_1 \rightarrow \infty$, the drag $Re(D_N)$ decreases as k_1 increases.

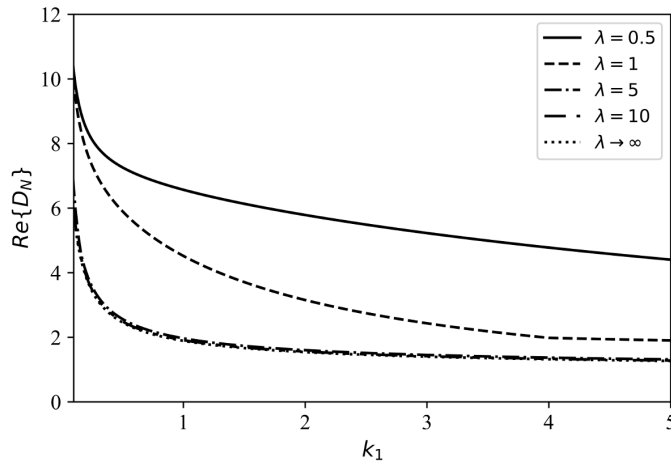


Fig. 6. Variation of real part of normalized drag D_N with k_1 for $\tau = -1$, $\beta_1 = 5$, and $a = 1$

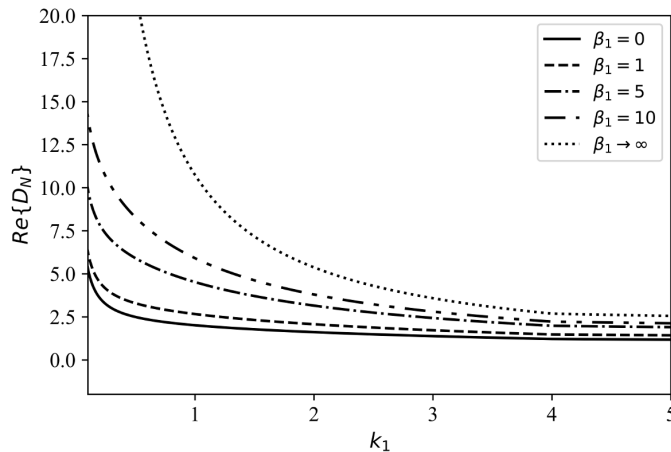


Fig. 7. Variation of real part of normalized drag D_N with k_1 for $\tau = -1$, $\lambda = 1$, and $a = 1$

8. Conclusions

We have obtained an analytical solution of the axisymmetric and steady flow of the couple stress fluid past a sphere embedded in a porous medium. The flow field is governed by Brinkman's equation in a porous medium. Stream function, pressure, couple stress components, and stress component expressions are presented. The drag force acting on the surface of the sphere in a porous medium is calculated. In special cases, we discussed some well-known cases. The effects of slip, couple stress, couple stress viscosity ratio, and permeability parameters on the drag are illustrated by graphs. From the figures, one can notice that:

- The drag force decreases as the couple stress parameter increases, and the drag acting on a slip sphere slightly increases as the couple stress viscosity ratio increases.
- The real part of drag increases as the slip parameter increases because fluid velocity is decreased on the surface of the sphere.
- For the consistent couple stress fluid, the drag force decreases if the couple stress parameter increases and the drag force increases as the slip parameter increases.

In future works, couple stress fluid past different geometric shapes with a slip effect in a porous medium may be investigated.

Appendix A

The constants given in Eqs. (25)–(27), Eq. (30) and Eq. (36) are defined as:

$$\begin{aligned}
 \xi_3 &= \xi_1 a, & \xi_4 &= \xi_2 a, \\
 H_1 &= K_{1/2}(\xi_1 a), & H_2 &= K_{3/2}(\xi_1 a), & H_3 &= K_{1/2}(\xi_2 a), & H_4 &= K_{3/2}(\xi_2 a), \\
 J_1 &= a\beta_1 + 2, & J_2 &= 3J_1 + a^2\alpha^2, \\
 J_3 &= \xi_3 H_1 J_1 + H_2 J_2, & J_4 &= \xi_4 H_3 J_1 + H_4 J_2, \\
 J_5 &= \xi_3 H_1 + 2H_2, & J_6 &= \xi_4^2 H_4 J_3 - \xi_3^2 H_2 J_4, \\
 J_7 &= \xi_4 H_3 + 2H_4, & J_8 &= \xi_3 H_1 J_1 + H_2 a^2 \alpha^2, \\
 J_9 &= \xi_4 H_3 J_1 + H_4 a^2 \alpha^2, & J_{10} &= \xi_4^2 H_4 J_8 - \xi_3^2 H_2 J_9, \\
 J_{11} &= (\tau + 2)H_4 + \xi_4 H_3, & J_{12} &= (\tau + 2)H_2 + \xi_3 H_1, \\
 J_{13} &= \xi_3 H_1 + H_2, & J_{14} &= \xi_4 H_3 + H_4, \\
 \Delta_1 &= \tau J_{10} + \xi_4^2 J_7 J_8 - \xi_3^2 J_5 J_9, \\
 \Delta_2 &= \xi_4^2 J_8 J_{14} - \xi_3^2 J_9 J_{13}.
 \end{aligned}$$

References

- [1] J. Bear. *Dynamics of fluids in porous media*. Courier Corporation, 2013.
- [2] H.C. Brinkman. A calculation of the viscous force exerted by a flowing fluid on a dense swarm of particles. *Flow, Turbulence and Combustion*, 1(1):27–34, 1949. doi: [10.1007/bf02120313](https://doi.org/10.1007/bf02120313).
- [3] R.H. Davis and H.A. Stone. Flow through beds of porous particles. *Chemical Engineering Science*, 48(23):3993–4005, 1993. doi: [10.1016/0009-2509\(93\)80378-4](https://doi.org/10.1016/0009-2509(93)80378-4).
- [4] B. Barman. Flow of a Newtonian fluid past an impervious sphere embedded in a porous medium. *Indian Journal of Pure and Applied Mathematics*, 27:1249–1256, 1996.
- [5] I. Pop and D.B. Ingham. Flow past a sphere embedded in a porous medium based on the Brinkman model. *International Communications in Heat and Mass Transfer*, 23(6):865–874, 1996. doi: [10.1016/0735-1933\(96\)00069-3](https://doi.org/10.1016/0735-1933(96)00069-3).
- [6] D. Srinivasacharya and J.V. Ramana Murthy. Flow past an axisymmetric body embedded in a saturated porous medium. *Comptes Rendus Mécanique*, 330(6):417–423, 2002. doi: [10.1016/s1631-0721\(02\)01478-x](https://doi.org/10.1016/s1631-0721(02)01478-x).

-
- [7] T. Grosan, A. Postelnicu, and I. Pop. Brinkman flow of a viscous fluid through a spherical porous medium embedded in another porous medium. *Transport in Porous Media*, 81(1):89–103, 2010. doi: [10.1007/s11242-009-9389-y](https://doi.org/10.1007/s11242-009-9389-y).
- [8] S. Deo and B.R. Gupta. Drag on a porous sphere embedded in another porous medium. *Journal of Porous Media*, 13(11):1009–1016, 2010. doi: [10.1615/JPorMedia.v13.i11.70](https://doi.org/10.1615/JPorMedia.v13.i11.70).
- [9] N.E. Leontev. Flow past a cylinder and a sphere in a porous medium within the framework of the Brinkman equation with the Navier boundary condition. *Fluid Dynamics*, 49(2):232–237, 2014. doi: [10.1134/S0015462814020112](https://doi.org/10.1134/S0015462814020112).
- [10] S. El-Sapa. Effect of permeability of Brinkman flow on thermophoresis of a particle in a spherical cavity. *European Journal of Mechanics-B/Fluids*, 79:315–323, 2020. doi: [10.1016/j.euromechflu.2019.09.017](https://doi.org/10.1016/j.euromechflu.2019.09.017).
- [11] M.S. Faltas, H.H. Sherief, A.A. Allam, and B.A. Ahmed. Mobilities of a spherical particle straddling the interface of a semi-infinite Brinkman flow. *Journal of Fluids Engineering*, 143(7):071402, 2021. doi: [10.1115/1.4049931](https://doi.org/10.1115/1.4049931).
- [12] M. Krishna Prasad and D. Srinivasacharya. Micropolar fluid flow through a cylinder and a sphere embedded in a porous medium. *International Journal of Fluid Mechanics Research*, 44(3):229–240, 2017. doi: [10.1615/InterJFluidMechRes.2017015283](https://doi.org/10.1615/InterJFluidMechRes.2017015283).
- [13] B.R. Jaiswal. A non-Newtonian liquid sphere embedded in a polar fluid saturated porous medium: Stokes flow. *Applied Mathematics and Computation*, 316:488–503, 2018. doi: [10.1016/j.amc.2017.08.009](https://doi.org/10.1016/j.amc.2017.08.009).
- [14] K. Ramalakshmi and P. Shukla. Drag on a fluid sphere embedded in a porous medium with solid core. *International Journal of Fluid Mechanics Research*, 46(3):219–228, 2019. doi: [10.1615/InterJFluidMechRes.2018025197](https://doi.org/10.1615/InterJFluidMechRes.2018025197).
- [15] K.P. Madasu and T. Bucha. Influence of mhd on micropolar fluid flow past a sphere implanted in porous media. *Indian Journal of Physics*, 95(6):1175–1183, 2021. doi: [10.1007/s12648-020-01759-7](https://doi.org/10.1007/s12648-020-01759-7).
- [16] V.K. Stokes. Couple stresses in fluids. In *Theories of Fluids with Microstructure*, pages 34–80. Springer, 1966. doi: [10.1007/978-3-642-82351-0_4](https://doi.org/10.1007/978-3-642-82351-0_4).
- [17] V.K. Stokes. *Theories of Fluids with Microstructure: An Introduction*. Springer Science & Business Media, 2012. doi: [10.1007/978-3-642-82351-0](https://doi.org/10.1007/978-3-642-82351-0).
- [18] D. Pal, N. Rudraiah, and R. Devanathan. A couple stress model of blood flow in the microcirculation. *Bulletin of Mathematical Biology*, 50(4):329–344, 1988. doi: [10.1007/BF02459703](https://doi.org/10.1007/BF02459703).
- [19] N.A. Khan, A. Mahmood, and A. Ara. Approximate solution of couple stress fluid with expanding or contracting porous channel. *Engineering Computations*, 30(3):399–408, 2013. doi: [10.1108/02644401311314358](https://doi.org/10.1108/02644401311314358).
- [20] D. Srinivasacharya and K. Kaladhar. Mixed convection flow of couple stress fluid in a non-Darcy porous medium with Soret and Dufour effects. *Journal of Applied Science and Engineering*, 15(4):415–422, 2012.
- [21] M. Devakar, D. Sreenivasu, and B. Shankar. Analytical solutions of couple stress fluid flows with slip boundary conditions. *Alexandria Engineering Journal*, 53(3):723–730, 2014. doi: [10.1016/j.aej.2014.06.005](https://doi.org/10.1016/j.aej.2014.06.005).
- [22] D. Srinivasacharya, N. Srinivasacharyulu, and O. Odelu. Flow of couple stress fluid between two parallel porous plates. *International Journal of Applied Mathematics*, 41(2).
- [23] E.A. Ashmawy. Drag on a slip spherical particle moving in a couple stress fluid. *Alexandria Engineering Journal*, 55(2):1159–1164, 2016. doi: [10.1016/j.aej.2016.03.032](https://doi.org/10.1016/j.aej.2016.03.032).
- [24] P. Aparna, P. Padmaja, N. Pothanna, and J.V. Ramana Murthy. Couple stress fluid flow due to slow steady oscillations of a permeable sphere. *Nonlinear Engineering*, 9(1):352–360, 2020. doi: [10.1515/nleng-2020-0021](https://doi.org/10.1515/nleng-2020-0021).

- [25] S.O. Adesanya, S.O. Kareem, J.A. Falade, and S.A. Arekete. Entropy generation analysis for a reactive couple stress fluid flow through a channel saturated with porous material. *Energy*, 93:1239–1245, 2015. doi: [10.1016/j.energy.2015.09.115](https://doi.org/10.1016/j.energy.2015.09.115).
- [26] A.R. Hassan. The entropy generation analysis of a reactive hydromagnetic couple stress fluid flow through a saturated porous channel. *Applied Mathematics and Computation*, 369:124843, 2020. doi: [10.1016/j.amc.2019.124843](https://doi.org/10.1016/j.amc.2019.124843).
- [27] S.I. Abdelsalam, J.X. Velasco-Hernández, and A.Z. Zaher. Electro-magnetically modulated self-propulsion of swimming sperms via cervical canal. *Biomechanics and Modeling in Mechanobiology*, 20(3):861–878, 2021. doi: [10.1007/s10237-020-01407-3](https://doi.org/10.1007/s10237-020-01407-3).
- [28] M.M. Bhatti, S.Z. Alamri, R. Ellahi, and S.I. Abdelsalam. Intra-uterine particle–fluid motion through a compliant asymmetric tapered channel with heat transfer. *Journal of Thermal Analysis and Calorimetry*, 144(6):2259–2267, 2021. doi: [10.1007/s10973-020-10233-9](https://doi.org/10.1007/s10973-020-10233-9).
- [29] A.R. Hadjesfandiari and G.F. Dargush. Polar continuum mechanics. *arXiv preprint arXiv:1009.3252*, 2010.
- [30] A.R. Hadjesfandiari and G.F. Dargush. Couple stress theory for solids. *International Journal of Solids and Structures*, 48(18):2496–2510, 2011. doi: [10.1016/j.ijsolstr.2011.05.002](https://doi.org/10.1016/j.ijsolstr.2011.05.002).
- [31] A.R. Hadjesfandiari, G.F. Dargush, and A. Hajesfandiari. Consistent skew-symmetric couple stress theory for size-dependent creeping flow. *Journal of Non-Newtonian Fluid Mechanics*, 196:83–94, 2013. doi: [10.1016/j.jnnfm.2012.12.012](https://doi.org/10.1016/j.jnnfm.2012.12.012).
- [32] A.R. Hadjesfandiari, A. Hajesfandiari, and G.F. Dargush. Skew-symmetric couple-stress fluid mechanics. *Acta Mechanica*, 226(3):871–895, 2015. doi: [10.1007/s00707-014-1223-0](https://doi.org/10.1007/s00707-014-1223-0).
- [33] C.L.M.H. Navier. Mémoires de l’Académie Royale des Sciences de l’Institut de France. *Royale des Sciences de l’Institut de France*, 1823.
- [34] I.M. Eldesoky, S.I. Abdelsalam, W.A. El-Askary, A.M. El-Refaey, and M.M. Ahmed. Joint effect of magnetic field and heat transfer on particulate fluid suspension in a catheterized wavy tube. *BioNanoScience*, 9(3):723–739, 2019. doi: [10.1007/s12668-019-00651-x](https://doi.org/10.1007/s12668-019-00651-x).
- [35] M.M. Bhatti and S.I. Abdelsalam. Thermodynamic entropy of a magnetized ree-eyring particle-fluid motion with irreversibility process: A mathematical paradigm. *Journal of Applied Mathematics and Mechanics/Zeitschrift für Angewandte Mathematik und Mechanik*, 101(6):e202000186, 2021. doi: [10.1002/zamm.202000186](https://doi.org/10.1002/zamm.202000186).
- [36] S. El-Sapa and N.S. Alsudais. Effect of magnetic field on the motion of two rigid spheres embedded in porous media with slip surfaces. *The European Physical Journal E*, 44(5):1–11, 2021. doi: [10.1140/epje/s10189-021-00073-2](https://doi.org/10.1140/epje/s10189-021-00073-2).
- [37] K.P. Madasu, M. Kaur, and T. Bucha. Slow motion past a spheroid implanted in a Brinkman medium: Slip condition. *International Journal of Applied and Computational Mathematics*, 7(4):1–15, 2021. doi: [10.1007/s40819-021-01104-4](https://doi.org/10.1007/s40819-021-01104-4).
- [38] J. Happel and H. Brenner. *Low Reynolds Number Hydrodynamics: with Special Applications to Particulate Media*. Springer Science & Business Media, 2012.
- [39] S. El-Sapa, E.I. Saad, and M.S. Faltas. Axisymmetric motion of two spherical particles in a brinkman medium with slip surfaces. *European Journal of Mechanics-B/Fluids*, 67:306–313, 2018. doi: [10.1016/j.euromechflu.2017.10.003](https://doi.org/10.1016/j.euromechflu.2017.10.003).
- [40] V.K. Stokes. Effects of couple stresses in fluids on the creeping flow past a sphere. *The Physics of Fluids*, 14(7):1580–1582, 1971. doi: [10.1063/1.1693645](https://doi.org/10.1063/1.1693645).